

# MO-SAE: Multi-Objective Stacked Autoencoders Optimization for Edge Anomaly Detection

Lizhao Zhang<sup>1</sup>, Shengsong Kong<sup>1</sup>, Tao Guo<sup>1</sup>, Shaobo Li<sup>1\*</sup>, Zhenzhou Ji<sup>1\*</sup>

**Abstract**—Stacked AutoEncoders (SAE) have been widely adopted in edge anomaly detection scenarios. However, the resource-intensive nature of SAE can pose significant challenges for edge devices, which are typically resource-constrained and must adapt rapidly to dynamic and changing conditions. Optimizing SAE to meet the heterogeneous demands of real-world deployment scenarios, including high performance under constrained storage, low power consumption, fast inference, and efficient model updates, remains a substantial challenge. To address this, we propose an integrated optimization framework that jointly considers these critical factors to achieve balanced and adaptive system-level optimization. Specifically, we formulate SAE optimization for edge anomaly detection as a multi-objective optimization problem and propose MO-SAE (Multi-Objective Stacked AutoEncoders). The multiple objectives are addressed by integrating model clipping, multi-branch exit design, and a matrix approximation technique. In addition, a multi-objective heuristic algorithm is employed to effectively balance the competing objectives in SAE optimization. Our results demonstrate that the proposed MO-SAE delivers substantial improvements over the original approach. On the x86 architecture, it reduces storage space and power consumption by at least 50%, improves runtime efficiency by no less than 28%, and achieves an 11.8% compression rate, all while maintaining application performance. Furthermore, MO-SAE runs efficiently on edge devices with ARM architecture. Experimental results show a 15% improvement in inference speed, facilitating efficient deployment in cloud–edge collaborative anomaly detection systems.

## I. INTRODUCTION

SAE (Stacked AutoEncoders) are widely adopted in anomaly detection, particularly in edge scenarios, due to its technical merits [1]. SAE offers efficient feature learning capabilities that enable automatic extraction of meaningful representations from raw data, and it does not rely on large amounts of labeled data. Compared to complex large-scale models, SAE operates with high efficiency, making it well-suited for long-term deployment on edge devices. However, the direct deployment of SAE presents several challenges, including operating under resource constraints, ensuring timely responses to real-time data, balancing multiple optimization objectives, and managing high communication costs, particularly in cloud–edge collaborative environments. Consequently, optimization becomes a critical step in deploying SAE for edge-based anomaly detection.

Corresponding authors: Shaobo Li (lishaobo@hit.edu.cn) and Zhenzhou Ji (jizhenzhou@hit.edu.cn)

<sup>1</sup>Lizhao Zhang (lizhaozhang@stu.hit.edu.cn), Shengsong Kong (shengsongkong@stu.hit.edu.cn), Shaobo Li and Zhenzhou Ji are with Faculty of computing, Harbin Institute of Technology, Harbin 150000, China.

<sup>2</sup>Tao Guo (gt8399@hit.edu.cn) with Office of Cyber Security and Informatization, Harbin Institute of Technology, Harbin 150000, China.

Researchers have conducted extensive studies on computational efficiency and optimization under resource constraints [2], with a focus on software-based approaches [21], [22], [24] due to the relatively high cost and complexity of hardware optimization [3]. *Knowledge distillation* was proposed to train compact networks by transferring knowledge from a larger, fully trained network, though it poses challenges such as determining the optimal scale of the smaller network and incurring additional retraining overhead [4], [5]. *Weight matrix transformation* employs low-rank decomposition [6] to reduce storage requirements and accelerate inference, but it necessitates that the corresponding weight matrix satisfy well-defined mathematical conditions [7]. *Parameter sharing* [8] reduces model size by mapping original parameters to a constrained set using clustering [9] or hashing [10], although it lacks comprehensive theoretical analysis [11]. *Parameter quantization* [12] replaces original parameters with low-precision counterparts to facilitate hardware acceleration [25], but its effectiveness is limited by the range of supported data types. *Model pruning* widely used in computer vision and pattern recognition, operates at various levels [14]–[16], [26], yet typically requires specialized hardware and additional retraining. Numerous classical anomaly detection models have been introduced, including NSIBF [17], GANF [18], OmniAnomaly [19], and LSTM [20]. However, these models typically ignore computational efficiency in resource-constrained scenarios. Some studies [28], [29] propose model partitioning across edge–cloud environments to skip optimization, but this incurs significant communication overhead.

Most existing methods prioritize improving a single predefined objective, often leading to undesirable trade-offs such as increased retraining overhead or communication burden. This underscores the need for a unified approach that can effectively balance multiple competing objectives in anomaly detection. To this end, the proposed MO-SAE addresses these issues by simultaneously considering multiple optimization objectives. The core concepts include: First, based on a progressive clipping test, we propose model clipping that eliminates the retraining process. Next, a multi-branch exit design is integrated to improve runtime efficiency and generalization performance across various scenarios. Then, after formulating SAE optimization as a multi-objective problem, we introduce a heuristic algorithm to achieve trade-offs among the competing objectives. Finally, based on the theoretical analysis of approximation computation principles, we propose a matrix approximation method using equal-width binning to optimize the model update process of SAE for edge anomaly detection.

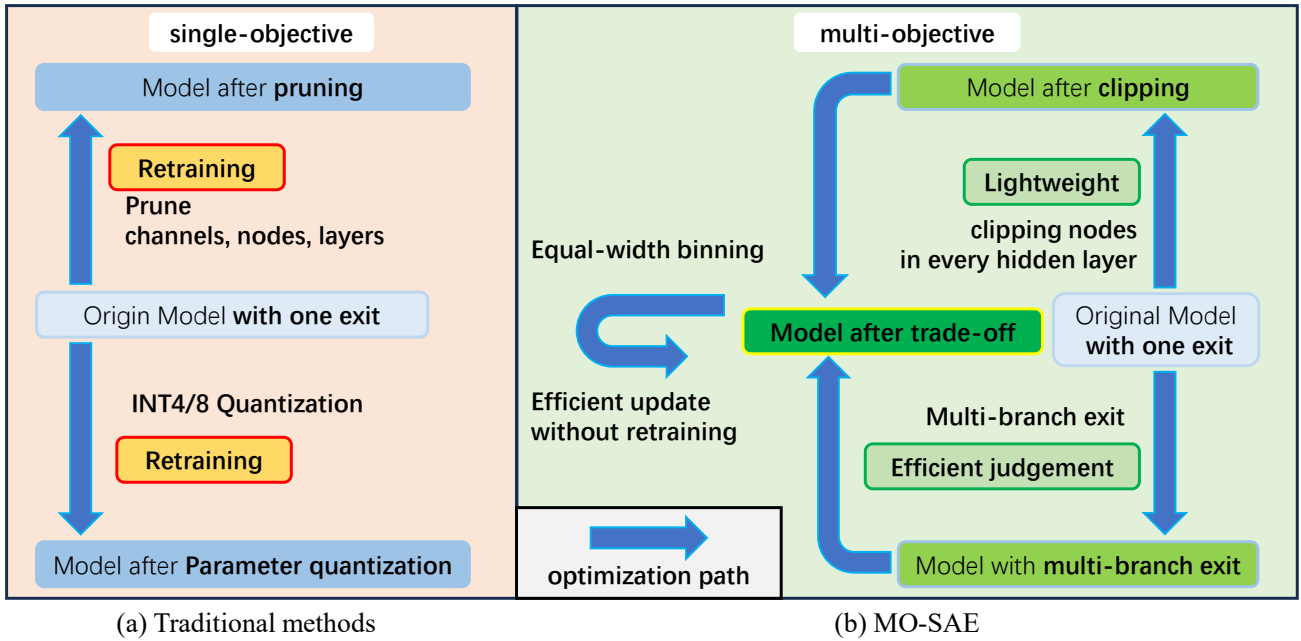


Fig. 1: Comparison between traditional methods and proposed MO-SAE.

The key contributions of this paper are summarized as follows:

- The proposed MO-SAE aims to enhance edge anomaly detection from multiple perspectives by cohesively incorporating multiple optimization methods, including model clipping, multi-branch exit design, and matrix approximation with equal-width binning.
- A multi-objective heuristic algorithm is employed to effectively balance multiple competing objectives in edge anomaly detection, including F1 score, runtime, storage space, and power consumption.
- Extensive experiments are conducted on the Credit Card Fraud and SMD datasets across both x86 and ARM architectures. The results show that the proposed MO-SAE can effectively improve the F1-based accuracy, reduces latency, and lowers storage space and power consumption on edge devices.

## II. MOTIVATION

Edge anomaly detection plays a crucial role in a wide range of real-world applications, such as financial fraud prevention, and real-time monitoring. SAE have emerged as a powerful unsupervised method due to their ability to learn compact representations of normal data and effectively identify anomalies. Although SAE serves as a foundational approach for anomaly detection, its practical application faces several critical challenges.

- Edge devices typically have constrained computational power, storage capacity, and battery life. SAEs contain a large number of parameters, demanding significant storage and computational resources.
- Edge anomaly detection requires real-time or near-real-time anomaly detection capabilities. SAE employ deep

neural network architectures to compute reconstruction errors layer-by-layer, which results in significant computational delay during inference.

- Addressing above challenges requires effective trade-offs among multiple optimization objectives, such as reducing resource consumption without significantly sacrificing application performance.
- Additionally, in scenarios like cloud-edge collaboration, SAE updating process is inevitable. Therefore, enhancing model update efficiency is a key challenge in SAE deployment on edge as well.

To address these challenges, this paper proposes MO-SAE, a multi-objective SAE optimization framework that minimizes resource consumption, enhances real-time detection, and improves model update efficiency for practical cloud-edge anomaly detection.

## III. METHOD AND FRAMEWORK

In this section, we present a detailed description of MO-SAE in the following three parts. First, MO-SAE is proposed by integrating model clipping, multi-branch exit design, and a matrix approximation technique, followed by in-depth comparisons with traditional methods. Second, we formulate the edge SAE as a multi-objective optimization problem and introduce a heuristic algorithm to balance competing objectives. Third, we utilize a matrix approximation technique to optimize the model update process. This is achieved by applying equal-width binning and approximate reconstruction to the original parameter matrix.

### A. Outline of Optimization Framework

Whether retraining is necessary for pruned deep learning models remains a debated issue in model optimization. For instance, models that are highly robust to structural

perturbations may require less or no additional retraining. However, many existing studies in model optimization do not evaluate a model’s robustness prior to optimization.

To address this issue, we adopt a progressive clipping test to evaluate whether the SAE for edge anomaly detection exhibits strong robustness to structural perturbations. In this study, the progressive clipping test utilizes a random sampling method to select neurons. The results of successive samplings are combined to generate a series of clipping schemes, covering mild to extreme levels of pruning, as illustrated in Fig. 2. Based on the analysis in Section IV-B, we propose three techniques to improve SAE for edge anomaly detection: model clipping (which eliminates retraining), multi-branch exit design (which improves runtime efficiency and generalization performance), and matrix approximation with equal-width binning (which optimizes model update process). The effectiveness of these techniques is demonstrated through comparisons between traditional methods and MO-SAE, as shown in Fig. 1. Specifically, the model clipping, illustrated in Fig. 3, focuses on pruning nodes within each hidden layer rather than pruning channels or entire layers. The multi-branch exit design, illustrated in Fig. 4, introduces multiple exits before the final output of the SAE. After data samples are fed into the model, the reconstruction error is computed at each possible exit and compared against a predefined reconstruction error threshold, thereby enhancing the runtime efficiency of edge anomaly detection. The model update optimization based on equal-width binning is further analyzed in Section III-C.

### B. Formulation and Algorithm

Our objective is to ensure that the optimized SAE delivers high application performance and runtime efficiency, while minimizing storage space and power consumption. Therefore, we formulate SAE optimization in edge anomaly detection as a multi-objective optimization problem and introduce a multi-objective heuristic algorithm to jointly optimize the model clipping and the multi-branch exit design, as illustrated in Algorithm 1 to manage trade-offs among conflicting optimization goals. The workflow is illustrated in Fig. 5. The multi-objective heuristic algorithm does not aggregate multiple objectives into a single weighted function. Instead, it uses non-dominated sorting to divide the population into different levels, thereby preserving a set of solutions that reflect various trade-offs among objectives. In brief, the multi-objective heuristic algorithm adopts the same selection, crossover, and mutation processes as the genetic algorithm, with two essential modifications. On one hand, the algorithm employs non-dominated sorting to rank individuals, ultimately generating populations with specialized capabilities to address varying task requirements. On the other hand, the selection probability is designed to satisfy two principles simultaneously. First, individuals from higher-ranked populations are more likely to be selected. Second, all individuals within the same population have an equal probability of selection. Specifically, assume that there are  $k$  selected non-dominated populations, denoted as  $Z_1, Z_2, \dots$ ,

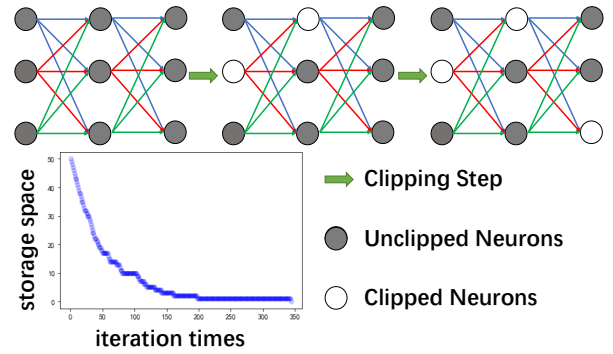


Fig. 2: Progressive clipping test.

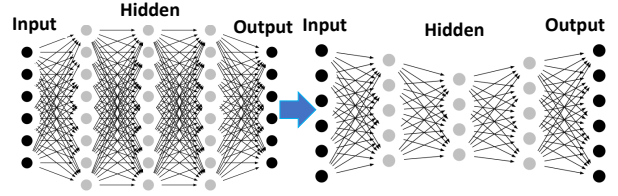


Fig. 3: Model clipping design.

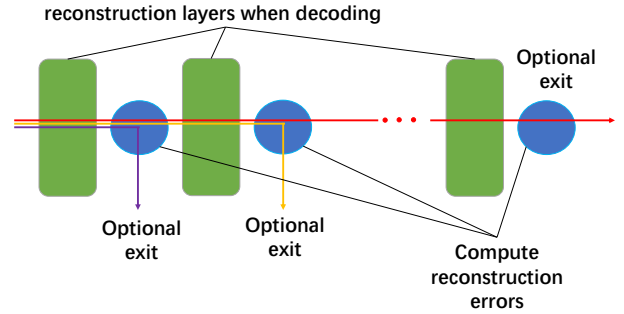


Fig. 4: Multi-branch exit design.

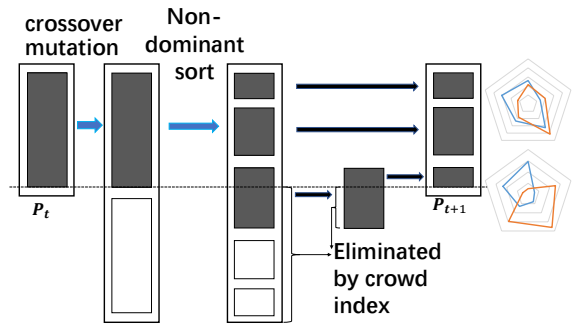


Fig. 5: Multi-objective heuristic algorithm workflow.

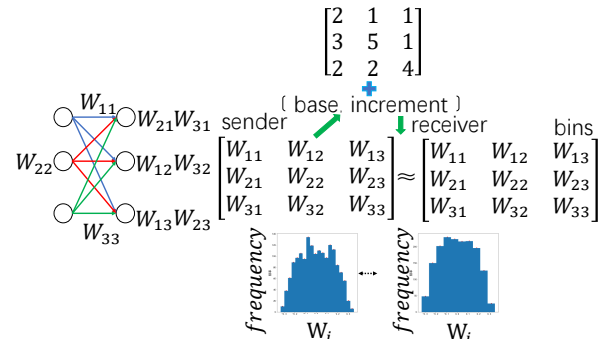


Fig. 6: Model update optimization in transmission process.

$Z_k$ . Here  $Z_i$  represents the  $i$ -th non-dominated population, and  $\text{count}(Z_i)$  denotes the number of individuals in  $Z_i$ . Thus, the selection probability for an individual is calculated as shown in Equation 1.

---

**Algorithm 1** proposed non-dominant sort

---

**Input:**  $P$ (the population set)  
**Output:**  $F_i$ (non-dominant sets at different grade)

```

1: function qdenomin(P)
2: for every p in P do
3:    $S_p = \emptyset$ 
4:    $n_p = 0$ 
5:   for every q in P do
6:     if q domin p then
7:       then add q to  $S_p$ 
8:     else
9:       if p domin q then
10:        then  $n_p = n_p + 1$ 
11:      end if
12:    end if
13:    if  $n_p = 0$  then
14:       $\text{Prank} = 1$ 
15:      add p to  $F_1$ 
16:    end if
17:  end for
18: end for
19: i=1
20: while  $F_i$  not empty do
21:    $Q = \emptyset$ 
22:   for every p in  $F_i$  do
23:     for every q in  $S_p$  do
24:        $n_p = n_p - 1$ 
25:       if  $n_p = 0$  then
26:          $\text{qrank} = i + 1$ 
27:         add q to Q
28:       end if
29:     end for
30:   end for
31:   i=i+1
32:    $F_i = Q$ 
33: end while
34: end function

```

---

$$\frac{1}{i} / \left( \sum_{i=1}^k \frac{1}{i} \cdot \text{count}(Z_i) \right) \quad (1)$$

We develop separate genetic information modules for the model clipping and the multi-branch exit design. For model clipping, the genetic information is encoded at the granularity of individual computational nodes in the hidden layers. Nodes marked for pruning are represented by 0, while those retained are represented by 1. For multi-branch exit design, the IEEE 754 floating-point format is adopted to encode different threshold percentages for reconstruction errors at each exit. For the combined case of the model clipping and the multi-branch exit design, the genetic information is formed by concatenating the two modules described above.

### C. Theoretical Analysis of Model Update Optimization

Approximate computing is a strategy that trades precision for efficiency within an acceptable error range, striving to balance accuracy, efficiency, and resource utilization. Specifically, we employ equal-width binning from matrix approximation to optimize the model update process. As

illustrated in Fig. 6, the model sender first determines the bin density—the number of partitions. The width of each bin is calculated based on the minimum and maximum values of the matrix. Each value is then mapped to its corresponding bin based on its magnitude, and the bin is used to represent the original value. This operation transforms continuous numerical data into several equal-width discrete bin values. Finally, the sender transmits three types of parameters derived from the binning process: base, increment, and step size. On the model receiver side, these parameters are used to reconstruct an approximate version of the original parameter matrix, enabling the inference process. To evaluate the effectiveness and feasibility of the approximate matrix, this study conducted a theoretical analysis, as outlined in Equations 2–7. Here,  $A$  represents the original matrix, approximated as  $(A + \Delta A)$ , and  $x$  is the true and unbiased input data, approximated as  $(x + \Delta x)$ . The error term  $\Delta A$  is introduced by the approximate matrix, while  $\Delta x$  arises from system measurement noise. In this context,  $\|\cdot\|$  denotes the 2-norm, so  $\|A\| \|A^{-1}\|$  is a fixed and well-defined value.

A good approximation requires satisfying the condition  $Ax = b$ , which is equivalent to  $(A + \Delta A)(x + \Delta x) = b$ . However, due to the inevitable presence of system measurement error  $\Delta x$ , the ideal case of  $Ax = b$  becomes unattainable. Instead, both  $A(x + \Delta x) = b$  and  $(A + \Delta A)(x + \Delta x) = b$  are approximations of the ideal scenario, differentiated by the distinct error terms. Based on the equivalence of  $Ax = b$  and  $(A + \Delta A)(x + \Delta x) = b$ , it can be inferred that both the approximate weight error  $\Delta A$ , introduced by the bin density, and the system measurement error  $\Delta x$ , can be treated as approximately zero matrices, thereby ensuring that the equation holds approximately. Since  $\Delta x$  is determined by the state of the input data, focusing on bin density becomes a reasonable strategy for optimizing model updates. As demonstrated in the subsequent derivations of inequalities, the infinitesimal relationship between  $\Delta x$  and  $\Delta A$  can be established. Assuming that the high-order terms of the system measurement error  $\Delta x$  are bounded, it follows that a good approximation can be achieved with a reasonable configuration of bin density for  $\Delta A$ .

$$(A + \Delta A)(x + \Delta x) = b \quad (2)$$

$$A\Delta x + \Delta Ax + \Delta A\Delta x = 0 \quad (3)$$

$$\Delta x = -A^{-1}(\Delta A)(x + \Delta x) \quad (4)$$

$$\|\Delta x\| \leq \|A^{-1}\| \|\Delta A\| \|x + \Delta x\| \quad (5)$$

$$\|\Delta x\| / \|x + \Delta x\| \leq \|A^{-1}\| \|\Delta A\| \|A\| / \|A\| \quad (6)$$

$$\|\Delta x\| \|A\| / \|x + \Delta x\| \|\Delta A\| \leq \|A\| \|A^{-1}\| \quad (7)$$

## IV. QUANTITATIVE EXPERIMENTS

### A. Datasets, Testbed and evaluation framework

To demonstrate the effectiveness, objectivity, and generality of the integrated optimization framework, quantitative experiments were conducted on real-world anomaly detection datasets. The SMD dataset contains per-minute operational data collected from 28 servers over a period of five weeks. It comprises 1,416,825 data entries with 38 features, among which 4.16% are labeled as anomalies. The Credit Card Fraud [23] dataset includes 284,807 European credit card transactions from September 2013, with 30 features and an anomaly rate of 0.17%.

This study uses an x86-based architecture to train and evaluate the optimized SAE model. The specific configuration consists of an Intel® Core™ i7-6700HQ CPU (2.60GHz), 8 GB of DDR4 2133MHz RAM, and an NVIDIA GeForce GTX 960M GPU (2GB). The NVIDIA® Jetson Xavier™, built on the ARM architecture, offers configurable modes with multiple power and core options. It is commonly used as an edge device. Thus, employing the NVIDIA® Jetson Xavier™ to validate the effectiveness of the solutions derived from the proposed optimization framework is well-suited for edge deployment scenarios.

To ensure a comprehensive evaluation of SAE in edge anomaly detection, the evaluation framework should be both generalizable and capable of demonstrating the effectiveness of optimization methods across diverse architectural platforms. This is achieved by using relative metrics rather than relying on absolute values. More unclipped neurons imply greater storage requirements; more basic operations lead to higher power consumption; and shorter runtime indicates better runtime efficiency. To evaluate the impact of model clipping and the multi-branch exit design, this study adopts three metrics—namely: the classic F1 score, running time, and compression rate—to assess application performance, runtime efficiency, and model update efficiency, respectively. Specifically, the compression rate is defined in Equation 8, where  $N$  represents the total number of parameter values. Maximum storage space and power consumption are normalized to enable comparison using relative values.

$$\text{compression rate} = ((\log_2 d_x / 8) \cdot N + 2 \cdot 8) / 8 \cdot N \quad (8)$$

### B. Analysis of Optimization Potential

On one hand, we aim to investigate the robustness of SAE in edge anomaly detection against structural perturbations caused by the model clipping. On the other hand, we explore the potential of optimizing SAE through the same model clipping technique and the previously introduced multi-branch exit design. To this end, we conducted experiments using the progressive clipping test and the Random Reconstruction Error Threshold (RRET) multi-branch exit design, respectively. In particular, the RRET multi-branch exit design sets exit thresholds for each branch by analyzing its reconstruction error distribution and selecting thresholds based

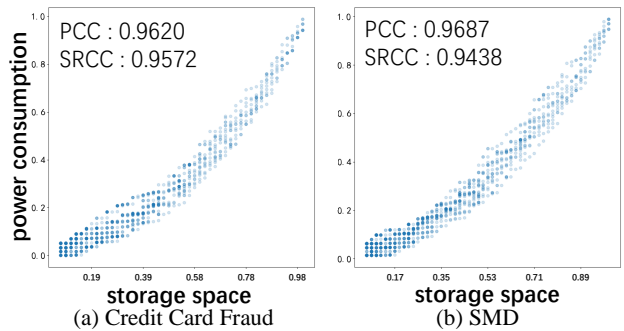


Fig. 7: Power consumption-Storage space Relationship.

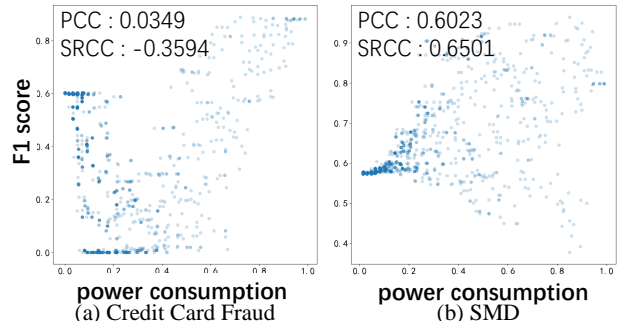


Fig. 8: Power consumption-F1 score Relationship.

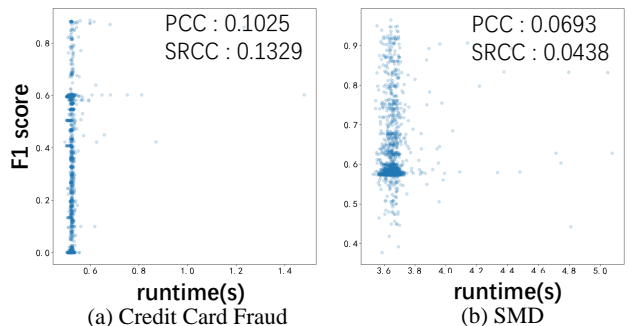


Fig. 9: Runtime-F1 score Relationship.

on randomly chosen quantiles. Based on these thresholds, it makes exit decisions on a per-sample basis. In contrast, the progressive clipping test is described in Section III-A. The experimental results are visualized using scatter plots, along with linear correlation analyses based on the Pearson Correlation Coefficient (PCC) and Spearman Rank Correlation Coefficient (SRCC), to illustrate the relationships among different optimization objectives.

Under the progressive clipping test, the relationships among optimization objectives exhibit varying patterns. As illustrated in Fig. 7, there is a strong linear correlation between storage space and power consumption. This aligns with intuition: More neurons required for SAE inference lead to higher computational load and, consequently, increased energy consumption. This suggests that the optimization objectives for storage space and power consumption are aligned under model clipping. The scatter data are relatively dispersed, and the linear correlation between power

consumption and F1 score is illustrated in Fig. 8. Notably, the scatter plot on the Credit Card Fraud dataset exhibits a segmented V-shaped correlation. This indicates a trade-off between the optimization objectives of achieving a high F1 score and minimizing power consumption. As illustrated in Fig. 9, the runtime remains within a fixed range and exhibits little variation with F1 score, indicating that model clipping is not effective in optimizing runtime efficiency.

The analysis of Figs. 10, 11, and 12 reveals that under the RRET multi-branch exit design, there exists a correlation between any two of the following objectives: runtime, power consumption, and F1 score. Given the study’s optimization goals—minimizing runtime and power consumption while maximizing F1 score—it is evident that significant trade-offs exist among these objectives. Another noteworthy observation is that the wide variation in F1 score suggests there is still room for improvement. The multi-branch exit design also proves effective in reducing runtime, thereby improving overall execution efficiency.

### C. Effective Trade-offs by Multi-objective Heuristic Algorithm

Quantitative experiments on both datasets present the results for the original SAE, MO-SAE without the model clipping, MO-SAE without the multi-branch exit design, and MO-SAE with both optimizations. The baseline models for Credit Card Fraud dataset include GRU, LSTM, SVM, KNN, ANN, and LSTM-Attention. The major reason for selecting these models is that they cover a wide range of machine learning paradigms, including traditional classification (SVM, KNN), shallow neural networks (ANN), recurrent neural networks (LSTM, GRU), and attention-based sequence models (LSTM-Attention). These models have demonstrated competitive performance in previous fraud detection research and are representative of different levels of model complexity and temporal modeling capabilities. DAGMM, LSTM-VAE, and OmniAnomaly are selected as representative baseline models for comparison on the SMD dataset, as they cover a spectrum of modeling paradigms—from static density estimation to temporal generative modeling—and allow for comprehensive evaluation of anomaly detection performance in multivariate time series under edge environments. As illustrated in Table I and Table II, bold font is used to indicate the top two values for each optimization objective, while underlines denote unacceptable F1 scores. MO-SAE employing a single optimization method—such as model clipping or multi-branch exit design—achieves an acceptable F1 score on one dataset but performs unsatisfactorily on the other. In contrast, when both optimizations are applied, MO-SAE not only maintains an acceptable F1 score on both datasets, but also achieves near-optimal performance in terms of storage space, power consumption, and runtime efficiency. The experimental analysis demonstrates that the combination of model clipping and the multi-branch exit design enables MO-SAE to achieve superior generalization across diverse scenarios, compared to using either model clipping or the multi-branch exit design

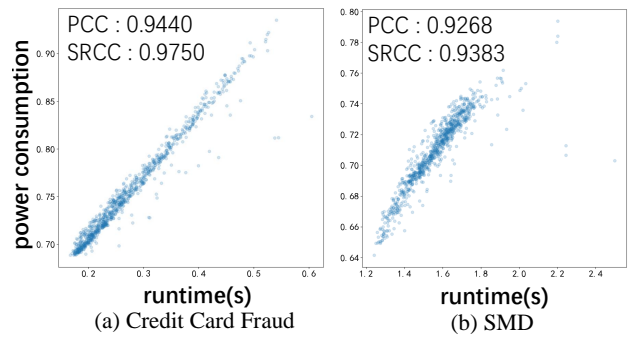


Fig. 10: Runtime-Power consumption Relationship.

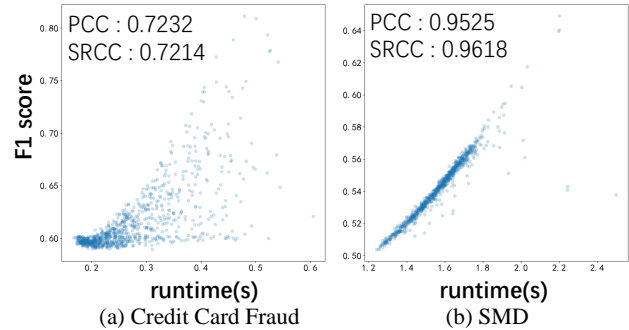


Fig. 11: Runtime-F1 score Relationship.

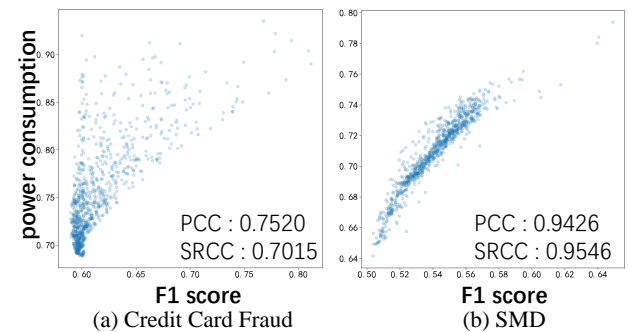


Fig. 12: F1 score-Power consumption Relationship.

alone. Overall, this joint approach ranks among the top two across key performance metrics. Furthermore, as illustrated in Table III and Table IV, validation on a single edge device under diverse ARM configurations confirms that the combination of model clipping and the multi-branch exit design allows MO-SAE to achieve robust performance while maintaining high efficiency, minimizing storage space and power consumption across both x86 and ARM platforms.

### D. Evaluation of Model Update Optimization

As illustrated in Fig. 14, the key to model update optimization via equal-width binning lies in selecting an appropriate bin density. A well-chosen bin density has a negligible impact on the model’s runtime, ensuring that the runtime optimization benefits discussed in IV-C are not compromised. As illustrated in Fig. 13, the F1 score increases gradually with the rising bin density and eventually reaches a plateau. An overly small bin density can lead to a significant decline

TABLE I: Performance comparison of different optimized schemes on Credit Card Fraud dataset.

Methods	F1 score	Storage space ratio	Runtime (s)	Power Consumption ratio
GRU [27]	0.78	–	–	–
LSTM [27]	0.79	12.35	21.90	49.46
SVM [27]	0.93	–	–	–
KNN [27]	0.07	–	–	–
ANN [27]	0.78	–	–	–
LSTM-attention [27]	<b>0.95</b>	12.37	19.35	49.55
Original	0.88	1.00	0.70	1.00
MO-SAE without Model clipping	0.85	1.00	<b>0.48</b>	0.92
MO-SAE without Multi-branch exit design	<u>0.60</u>	<b>0.10</b>	0.57	<b>0.04</b>
MO-SAE	<b>0.91</b>	<b>0.31</b>	<b>0.44</b>	<b>0.18</b>

TABLE II: Performance comparison of different optimized schemes on SMD dataset.

Methods	F1 score	Storage space ratio	Runtime (s)	Power Consumption ratio
DAGMM [19]	0.70	–	–	–
LSTM-VAE [19]	0.78	–	–	–
OmniAnomaly [19]	0.88	831.01	128.63	1093069.97
Original	0.79	1.00	4.88	1.00
MO-SAE without Model clipping	<u>0.63</u>	1.00	<b>2.05</b>	0.77
MO-SAE without Multi-branch exit design	<b>0.95</b>	<b>0.45</b>	3.92	<b>0.49</b>
MO-SAE	<b>0.92</b>	<b>0.47</b>	<b>3.49</b>	<b>0.37</b>

TABLE III: Performance comparison on Credit Card Fraud dataset under real resource-limited intelligent platform.

Method	F1 Score	Runtime (s) under different Work modes				
		15w, 2cores	15w, 4cores	15w, 6cores	10w, 2cores	10w, 4cores
Original	<b>0.88</b>	1.60	2.03	2.07	1.88	2.35
MO-SAE without Model clipping	0.85	<b>1.34</b>	<b>1.76</b>	<b>1.73</b>	<b>1.65</b>	<b>2.07</b>
MO-SAE without Multi-branch exit design	<u>0.60</u>	1.57	2.00	2.05	1.83	2.36
MO-SAE	<b>0.91</b>	<b>1.16</b>	<b>1.54</b>	<b>1.52</b>	<b>1.45</b>	<b>1.83</b>

TABLE IV: Performance comparison on SMD dataset under real resource-limited intelligent platform.

Method	F1 Score	Runtime (s) under different Work modes				
		15w, 2cores	15w, 4cores	15w, 6cores	10w, 2cores	10w, 4cores
Original	0.79	10.29	13.73	13.86	13.29	16.59
MO-SAE without Model clipping	<u>0.63</u>	<b>5.58</b>	<b>7.44</b>	<b>7.47</b>	<b>7.15</b>	<b>9.01</b>
MO-SAE without Multi-branch exit design	<b>0.95</b>	10.21	13.67	13.73	13.06	16.48
MO-SAE	<b>0.92</b>	<b>8.87</b>	<b>11.88</b>	<b>11.81</b>	<b>11.33</b>	<b>13.28</b>

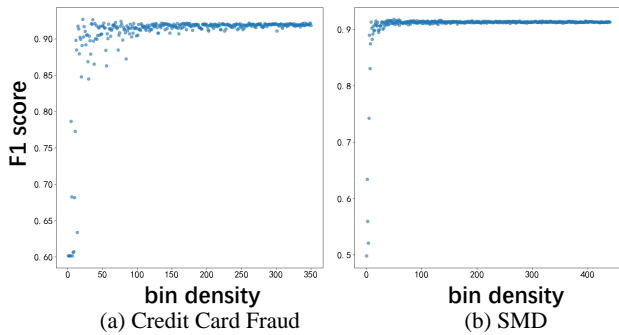


Fig. 13: Variation of F1 score with Increasing bin density.

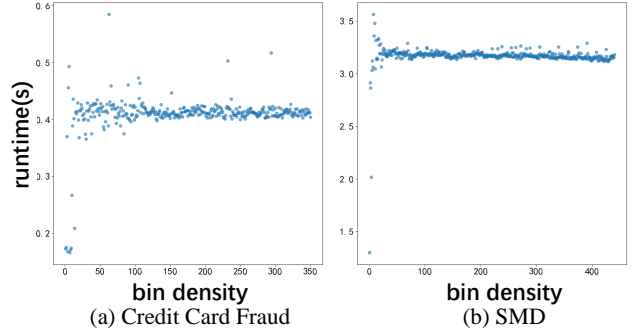


Fig. 14: Variation of runtime with Increasing bin density.

in model performance, while an excessively large bin density may result in unnecessary bandwidth waste and model update inefficiency, especially in cloud-edge collaboration scenarios. To ensure MO-SAE delivers stable performance, this study

sets bin density to 100 for both datasets, achieving an 11.08% compression rate compared to the original.

## V. CONCLUSIONS

In this paper, we propose an integrated optimization framework that systematically optimizes SAE from multiple aspects, including application performance, storage space, power consumption, runtime efficiency, and model update efficiency. Based on model clipping and a multi-branch exit design, we introduce a multi-objective heuristic algorithm to balance trade-offs among competing optimization objectives. Additionally, grounded in solid theoretical analysis and quantitative experiments results, we develop model update optimization tailored for the transmission process. Extensive experiments on real-world datasets validate the effectiveness of MO-SAE.

## ACKNOWLEDGMENT

This work was supported by National Natural Science Foundation of China under Grant No. 62406087, Shandong Natural Science Foundation of China under Grant No. ZR2024QF139, State Key Laboratory of Processors (ICT, CAS) under Grant No. CLQ202406, and State Key Laboratory of Computer Architecture (ICT,CAS) under Grant No. CARCHA202104.

## REFERENCES

- [1] D. Liu, Y. Wang, C. Liu, X. Yuan, C. Yang, and W. Gui, "Data model related interpretable transformer network for predictive modeling and key sample analysis in industrial processes," *IEEE Trans. Ind. Inf.*, vol. 19, no. 9, pp. 9325–9336, Sep. 2023. doi: 10.1109/TII.2022.3227731
- [2] L. Liu, G. G. Yen, and Z. He, "EvolutionViT: Multi-objective evolutionary vision transformer pruning under resource constraints," *Information Sciences*, vol. 689, Art. no. 121406, Jan. 2025. doi: 10.1016/j.ins.2024.121406
- [3] H. Cheng, M. Zhang, and J. Shi, "A survey on deep neural network pruning: Taxonomy, comparison, analysis, and recommendations," *IEEE Trans. Pattern Anal. Mach. Intell.*, 2024, early access.
- [4] S. Thomine and H. Snoussi, "Dual model knowledge distillation for industrial anomaly detection," *Pattern Anal. Appl.*, vol. 27, Art. no. 77, 2024. doi: 10.1007/s10044-024-01295-8
- [5] S. Li, T. Su, X.-Y. Zhang, and Z. Wang, "Continual learning with knowledge distillation: A survey," *IEEE Trans. Neural Netw. Learn. Syst.*, vol. 35, no. 1, pp. 1–21, 2024. doi: 10.1109/TNNLS.2024.3476068
- [6] A. Novikov, D. Podoprikin, A. Osokin, and D. P. Vetrov, "Tensorizing neural networks," in *Proc. 29th Int. Conf. Neural Inf. Process. Syst. (NeurIPS)*, Montreal, Canada, 2015, pp. 442–450.
- [7] P. Wang and J. Cheng, "Accelerating convolutional neural networks for mobile applications," in *Proc. 24th ACM Int. Conf. Multimedia (ACM MM)*, Amsterdam, The Netherlands, Oct. 2016, pp. 541–545. doi: 10.1145/2964284.2967280
- [8] W. Chen, J. Wilson, S. Tyree, K. Q. Weinberger, and Y. Chen, "Compressing convolutional neural networks in the frequency domain," in *Proc. 22nd ACM SIGKDD Int. Conf. Knowl. Discov. Data Min. (KDD)*, San Francisco, CA, USA, Aug. 2016, pp. 1475–1484. doi: 10.1145/2939672.2939839
- [9] J. Wu, Y. Wang, Z. Wu, Z. Wang, A. Veeraraghavan, and Y. Lin, "Deep  $k$ -means: Re-training and parameter sharing with harder cluster assignments for compressing deep convolutions," *arXiv preprint arXiv:1806.09228*, Jun. 2018. doi: 10.48550/arXiv.1806.09228
- [10] W. Chen, J. T. Wilson, S. Tyree, K. Q. Weinberger, and Y. Chen, "Compressing neural networks with the hashing trick," in *Proc. 32nd Int. Conf. Mach. Learn. (ICML)*, Lille, France, Jul. 2015, pp. 2285–2294.
- [11] J. Frankle and M. Carbin, "The lottery ticket hypothesis: Finding sparse, trainable neural networks," in *Proc. 7th Int. Conf. Learn. Represent. (ICLR)*, May 2019. Available: <https://openreview.net/forum?id=rJl-b3RcF7>
- [12] D. Soudry, I. Hubara, and R. Meir, "Expectation backpropagation: Parameter-free training of multilayer neural networks with continuous or discrete weights," in *Proc. 28th Int. Conf. Neural Inf. Process. Syst. (NeurIPS)*, Montreal, Canada, Dec. 2014, pp. 963–971.
- [13] F. Yu, K. Huang, M. Wang, Y. Cheng, W. Chu, and L. Cui, "Width & depth pruning for vision transformers," in *Proc. AAAI Conf. Artif. Intell.*, vol. 36, no. 3, pp. 3143–3151, Jun. 2022. doi: 10.1609/aaai.v36i3.20222
- [14] S. Lin, R. Ji, Y. Li, C. Deng, and X. Li, "Towards compact ConvNets via structure-sparsity regularized filter pruning," *arXiv preprint arXiv:1901.07827*, Mar. 2019. doi: 10.48550/arXiv.1901.07827
- [15] D. Mehta, K. I. Kim, and C. Theobalt, "On implicit filter level sparsity in convolutional neural networks," in *Proc. IEEE/CVF Conf. Comput. Vis. Pattern Recognit. (CVPR)*, Long Beach, CA, USA, Jun. 2019, pp. 520–528. doi: 10.1109/CVPR.2019.00061
- [16] S. Li, K. Osawa, and T. Hoefer, "Efficient quantized sparse matrix operations on tensor cores," in *Proc. SC22: Int. Conf. High Perform. Comput., Netw., Storage and Anal.*, Dallas, TX, USA, Nov. 2022, pp. 1–15. doi: 10.1109/SC41404.2022.00042
- [17] C. Feng and P. Tian, "Time series anomaly detection for cyber-physical systems via neural system identification and Bayesian filtering," in *Proc. 27th ACM SIGKDD Conf. Knowl. Discov. Data Min. (KDD)*, Virtual Event, Singapore, Aug. 2021, pp. 2858–2867. doi: 10.1145/3447548.3467137
- [18] E. Dai and J. Chen, "Graph-augmented normalizing flows for anomaly detection of multiple time series," *arXiv preprint arXiv:2202.07857*, May 2022. doi: 10.48550/arXiv.2202.07857
- [19] Y. Su, Y. Zhao, C. Niu, R. Liu, W. Sun, and D. Pei, "Robust anomaly detection for multivariate time series through stochastic recurrent neural network," *arXiv preprint arXiv:1802.09587*, 2019. Available: <https://arxiv.org/abs/1802.09587>
- [20] K. Hundman, V. Constantinou, C. Laporte, I. Colwell, and T. Soderstrom, "Detecting spacecraft anomalies using LSTMs and nonparametric dynamic thresholding," in *Proc. 24th ACM SIGKDD Int. Conf. Knowl. Discov. Data Min. (KDD)*, London, U.K., Jul. 2018, pp. 387–395. doi: 10.1145/3219819.3219845
- [21] R. Han, Q. Zhang, C. H. Liu, G. Wang, J. Tang, and L. Y. Chen, "LegoDNN: Block-grained scaling of deep neural networks for mobile vision," in *Proc. 27th Annu. Int. Conf. Mobile Comput. Netw. (MobiCom)*, New Orleans, LA, USA, Oct. 2021, pp. 406–419. doi: 10.1145/3447993.3483249
- [22] Z. Zhao, K. M. Barijough, and A. Gerstlauer, "Network-level design space exploration of resource-constrained networks-of-systems," *ACM Trans. Embed. Comput. Syst.*, vol. 19, no. 4, pp. 1–26, Jul. 2020. doi: 10.1145/3387918
- [23] E. Ileberi, Y. Sun, and Z. Wang, "A machine learning based credit card fraud detection using the GA algorithm for feature selection," *J. Big Data*, vol. 9, no. 1, Art. no. 24, Dec. 2022. doi: 10.1186/s40537-022-00573-8
- [24] S. Teerapittayanon, B. McDanel, and H. T. Kung, "BranchyNet: Fast inference via early exiting from deep neural networks," *arXiv preprint arXiv:1709.01686*, Sep. 2017. doi: 10.48550/arXiv.1709.01686
- [25] K. Wang, Z. Liu, Y. Lin, J. Lin, and S. Han, "HAQ: Hardware aware automated quantization with mixed precision," in *Proc. IEEE/CVF Conf. Comput. Vis. Pattern Recognit. (CVPR)*, Long Beach, CA, USA, Jun. 2019, pp. 8604–8612. doi: 10.1109/CVPR.2019.00881
- [26] H. Mao, S. Han, J. Pool, and W. J. Dally, "Exploring the granularity of sparsity in convolutional neural networks," in *Proc. IEEE Conf. Comput. Vis. Pattern Recognit. Workshops (CVPRW)*, Honolulu, HI, USA, Jul. 2017, pp. 1927–1934. doi: 10.1109/CVPRW.2017.241
- [27] I. Benchaji, S. Douzi, B. El Ouahidi, and J. Jaafari, "Enhanced credit card fraud detection based on attention mechanism and LSTM deep model," *J. Big Data*, vol. 8, no. 1, Art. no. 151, Dec. 2021. doi: 10.1186/s40537-021-00541-8
- [28] L. Yang, X. Shen, C. Zhong, and Y. Liao, "On-demand inference acceleration for directed acyclic graph neural networks over edge-cloud collaboration," *J. Parallel Distrib. Comput.*, vol. 171, pp. 79–87, Jan. 2023. doi: 10.1016/j.jpdc.2022.09.005
- [29] J. Tian, X. Li, and X. Qin, "Reinforcement learning based collaborative inference and task offloading optimization for cloud-edge-end systems," in *Proc. 2024 Int. Joint Conf. Neural Netw. (IJCNN)*, Yokohama, Japan, Jun. 2024, pp. 1–8. doi: 10.1109/IJCNN60899.2024.10651115